DOI: 10.1002/ejic.200600299

A Density Functional Study of the Hydrogenation of Ketones Catalysed by Neutral Rhodium-Diphosphane Complexes

Francine Agbossou-Niedercorn*[a] and Jean-François Paul*[b]

Keywords: Density functional calculations / Hydrogenation / Ketones / Rhodium / Asymmetric catalysis

The potential energy profile of Rh^I-catalysed hydrogenation of ketones has been computed for the simple model system [Rh{$H_3POCH_2CH_2N(H)PH_3$}(Cl)] using DFT calculations. The general sequence of the catalytic cycle involves coordination of the carbonyl derivative to the neutral Rh^I complex followed by oxidative addition of molecular hydrogen providing rhodium dihydride intermediates. The latter are converted into alkoxy hydrides by a migratory insertion reaction. Reductive elimination of the alcohol and substitution of the latter by the incoming substrate completes the catalytic cycle. Intermediates and transition states of all catalytic steps have been located. Two isomeric derivatives bearing the model substrate have been found for the [Rh{$H_3POCH_2CH_2N(H)PH_3$}(Cl)(H_2CO)] complex. Eight diastereomeric pathways have been followed for the *cis* addition of molecular hydrogen to [Rh{$H_3POCH_2CH_2N(H)PH_3$}(Cl)(H_2CO)] leading to eight distinct isomeric dihydride intermediates. Four dihydride complexes can be considered as the more accessible compounds. The site preference for migratory insertion and transition states discriminates the main path of the catalytic reaction. Migratory insertion to form the alkoxy hydride constitute the turn over limiting step of the process. The potential energy profile has been found to be smooth without excessive activation barriers.

Introduction

The enantioselective hydrogenation of prochiral ketones, which is one of the most exiting and powerful methods of synthesising chiral alcohols, has been receiving increased attention and has led to notable successes.[1] When ruthenium-based catalysts have been applied in the enantioselective hydrogenation of prochiral ketones,[2] rhodium complexes have proven to lead to very efficient processes along with potential industrial applications.[2–4] Likewise, asymmetric transfer hydrogenation of ketones has been well investigated over the last few decades[5], prompted by the very important contribution of Noyori's group.[6]

The most actively explored asymmetric hydrogenation mechanism has been the enantioselective hydrogenation of C=C bonds catalysed by cationic Rh^I-diphosphane complexes. Chemical,[7–14] kinetic[9] and theoretical[15,16] studies have been carried out. As a result, the rhodium-catalysed hydrogenation of dehydroamino acids leading to enantiomerically pure α-amino acids is considered to be a thoroughly understood reaction based on work carried out in the research groups of Halpern[7] and Brown[8] who revealed the underlying steps of the process. It has been demonstrated that the minor diastereomer resulting from the coordination of the enamide to the cationic Rh-diphosphane precursor reacts more rapidly with molecular hydrogen providing the observed prevailing hydrogenated product.[9–13] However, the reason for this increased reactivity is still not clearly understood. In addition, a complete understanding of the stereoselection has not yet been achieved. Finally, as highlighted recently by Rossen,[17] this classical mechanism of Rh-catalysed hydrogenation might not definitely be valid for all bisphosphane and metal combinations.

Much effort has been devoted to characterising transient intermediates in the C=C hydrogenation reactions. Among them, the cationic Rh-diphosphane-enamide complex[7,10,14] and the alkyl monohydride species[8,12] have been characterised by various spectroscopic and X-ray-based methods. Also, the presumed dihydride intermediate has been investigated by PHIP (*para*-hydrogen induced polarisation) NMR spectroscopy, which is a powerful tool for studying hydrogenation reactions.[18] Thus, while utilising *para*-hydrogen and appropriate complexes, elusive species could be detected. In this way, Selke and Bargon[19] observed a rhodium dihydride complex while using a sugar-based bisphosphinite ligand (Scheme 1). More recently, Bargon and Brown[20] reported the observation of an agostic complex which is encountered on the path of hydride transfer to the coordinated substrate (Scheme 1).

[a] Unité Catalyse et Chimie du Solide UMR CNRS 8181, ENSCL-CHIMIE, Bat C7,
B. P. 90108, 59652 Villeneuve d'Ascq Cedex, France
Fax: +33-3-20436585
E-mail: francine.agbossou@ensc-lille.fr
[b] Université des Sciences et Technologies de Lille, C3
Fax: +33-3-20436165,
E-mail: Jean-Francois.paul@univ-lille1.fr

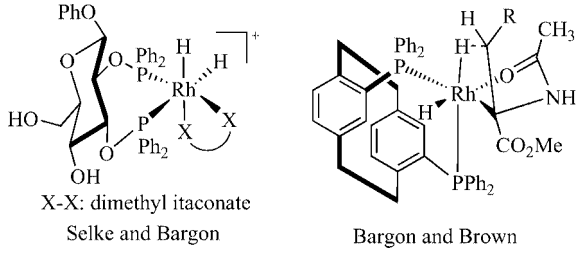

Scheme 1. Characterised dihydride-Rh complexes.

A second mechanism of hydrogenation that has been studied to some extent is related to the transfer hydrogenation of C=O bonds catalysed by Rh^{I}[21,22] and Ru^{II} complexes.[23] However, much less is known about the mechanism of the molecular hydrogen-based hydrogenation of ketones catalysed by rhodium species. Although the catalytic results are quite satisfactory in terms of efficiency, little is known experimentally about intermediates and reaction steps and the reaction mechanism has not been elucidated so far. Nevertheless, mechanistic hypotheses have been made in order to take into account the several experimental observations. Primarily, Schrock and Osborn[24] proposed a mechanism for the hydrogenation of ketones catalysed by cationic rhodium complexes bearing basic monophosphanes. One step of the catalytic cycle is an oxidative addition of molecular hydrogen providing a rhodium-dihydride complex. The reported catalytic system is promoted by small quantities of water (ca. 1% of H_2O). A study carried out either in the presence of D_2 or D_2O gave rise to a mechanism involving an active participation of water that would account for the determined incorporation of deuterium from D_2O. Actually, the key points are (1) the participation of a rhodium dihydride intermediate and (2) the promotion of the second hydrogen atom transfer by the small quantity of water as depicted in Scheme 2.

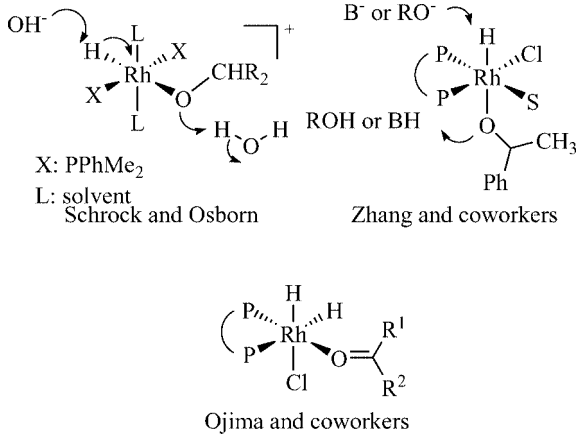

Scheme 2. Examples of reported rhodium-hydride intermediates.

More recently, Zhang[25] proposed a mechanism to take into account the beneficial effect provided by the use of amines which promoted both the activity and selectivity (Δee up to 38%) of the hydrogenation of simple ketones. In the catalytic cycle, an oxidative addition of molecular hydrogen on the rhodium precursor is considered prior to substrate coordination followed by hydride transfer to the coordinated substrate (Scheme 2). Yet, the reaction is carried out in methanol and the possibility of cationic rhodium catalytic intermediates has not been envisioned, the proposed mechanism being based only on noncharged intermediates.

Ojima described the efficient enantioselective hydrogenation of α-keto esters catalysed by neutral Rh–BPPM complexes [BPPM: (2*S*,4*S*)-*N*-*tert*-butoxycarbonyl-4-(diphenylphosphanyl)-2-[(diphenylphosphanyl)methyl]pyrrolidine][26] and proposed a mechanism based on results obtained while varying the solvent.[27] Dry aprotic solvents bestowed the best results both in terms of activity and enantioselectivity. These authors propose that both hydrides (Scheme 2) resulting from the oxidative addition of hydrogen onto the Rh–substrate adduct are successively transferred to the substrate. Meaningfully, it has been suggested that a retention of chloride on rhodium might be the clue for the increased efficiency of the catalyst.

In previous studies, we have shown that the enantioselective hydrogenation of functionalised ketones can be carried out very efficiently in the presence of neutral rhodium precursors bearing aminophosphane phosphinite ligands (AMPP).[28] The potential of such ligands has further been assayed in the highly enantioselective hydrogenation of fluorinated ketones including simple ketones.[29] We have also reported on the use of a combination of molecular mechanics-based methods and extended Hückel calculations in order to have access to the most stable catalytic intermediates and to their reactivity.[30]

Modern efforts have emphasised the potential of computational methods for organometallic catalysis investigations.[31] We became interested in using such methods to examine the catalytic cycle of the hydrogenation of ketones assisted by rhodium-aminophosphanephosphinite catalysts. To address the catalytic cycle, several computational approaches are possible. One deals with the general mechanism and the associated energetic profile while considering neutral catalytic intermediates and a second deals with the quest of the enantiodetermining step of the cycle. Both types of information require different levels of computation and consequently different ranges of calculation times. The aim of this study was to obtain an insight into the most probable energy profile of the catalytic cycle of ketone hydrogenation involving neutral rhodium diphosphane catalysts. Such an approach has not been undertaken to the best of our knowledge. Here, we report on the results of DFT computations of the catalytic reaction potential energy surface for a simple achiral aminophosphane phosphinite-based model system. In this paper, we describe the model system used, the computational method applied, and the overall reaction pathways explored.

Background and Calculation Methods

Despite our many attempts, we were unable to characterise, by NMR, catalytic intermediates under our classical ketone hydrogenation conditions (room temperature, 1 atm H_2, toluene). Indeed, only the starting rhodium dimeric complexes of the type $[Rh\{AMPP\}Cl]_2$ could be observed by ^{31}P NMR spectroscopy. However, the hydrogenation experiments carried out under various catalytic conditions did provide evidence for the participation of neutral intermediates bearing the chiral diphosphane along with a nonchiral ancillary ligand. For example, when the hydrogenation of benzylbenzoylformamide was run in ethanol in the presence of a cationic precatalyst, a slow reaction ($t_{1/2}$ = 4 h) with a very low *ee* was achieved (5.5% *ee*) (Table 1, entry 1).[32]

Table 1. Enantioselective hydrogenation of benzylbenzoylformamide.[a]

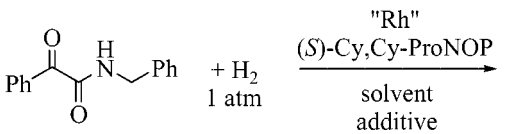

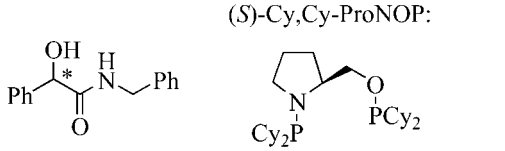

Cy: cyclohexyl

Entry	"Rh"	Solvent	Additive	$t_{1/2}$ [min][b]	*ee* (%) (conf.)
1	$[Rh(COD)_2]BF_4$	EtOH	–	240	5.5 (*R*)
2	$[Rh(COD)Cl]_2$	EtOH	–	28	64.8 (*S*)
3	$[Rh(COD)Cl]_2$	toluene	–	20	74 (*S*)
4	$[Rh(COD)I]_2$[c]	toluene	–	25	67 (*S*)
5	$[Rh(COD)_2]BF_4$	toluene	–	n.d.[d]	3 (*S*)
6	$[Rh(COD)_2]BF_4$	toluene	LiBr	18	69 (*S*)
7	$[Rh(COD)_2]BF_4$	toluene	LiI	40	62.2 (*S*)

[a] Substrate/Rh = 200:1. [b] Time of half conversion of the substrate. [c] F. Agbossou-Niedercorn, unpublished results. [d] n.d.: not determined, substrate/Rh = 45:1, total conversion after 3 d.

Interestingly, if the hydrogenation occurs in ethanol in the presence of a neutral precursor, an enhanced efficiency is attained as the chiral alcohol is produced in ca. 65% *ee* and with a higher rate ($t_{1/2}$ = 28 min) (Table 1, entry 2). The behaviour of diphosphane-rhodium complexes in various solvents deserves some comment. For instance, the reaction of neutral rhodium complexes with an amidophosphane phosphinite results in the formation of a mixture of cationic and neutral compounds in methanol, as shown by Pregosin.[33] Also, an earlier study of Bakos[34] outlined the behaviour of complexes of type "$Rh(P_2)$(diolefin)Cl" in various solvents (dichloromethane, benzene, methanol). Equilibrium between a cationic and a neutral complex could account for the ^{31}P NMR features of the corresponding solution. Therefore, the efficiency improvement observed while comparing the two above-mentioned hydrogenations can be reasonably related to the active participation of neutral catalytic species. As further evidence, a reaction carried out in toluene with a neutral precatalyst provides the alcohol with 74 and 67% *ee* and with higher rates for Cl and I, respectively (Table 1, entries 3 and 4). This compares well with hydrogenations carried out while using a cationic precatalyst in toluene in the presence of either LiI or LiBr (Table 1, compare entries 7 and 4). This is consistent with retention of the halide on the catalytic intermediates throughout the entire process. The weak dielectric constant of aromatic solvents is in favour of retention of the halide on the rhodium during catalysis.[35] Finally, note that the reaction performed with a cationic precursor in toluene proceeds with a low rate and an extremely low enantioselectivity (Table 1, entry 5).

Additional earlier results prove the benefit obtained when the hydrogenations of ketopantolactone are performed in the presence of neutral rhodium-halide complexes in toluene, essentially on the enantioselectivity (compare all entries of Table 2).[36] As a matter of fact, 98% *ee* was reached for Rh-iodide-based catalysts.

Table 2. Effect of the ancillary ligand on asymmetric hydrogenation of ketopantolactone.

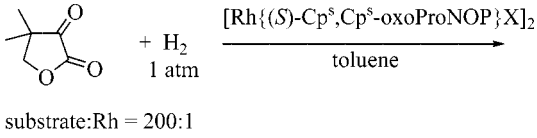

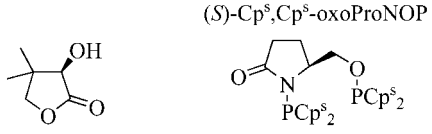

Cp^s: cyclopentyl

Entry	Precatalyst	$t_{1/2}$ [min]	*ee* (%) (conf.)
8	$[Rh(COD)_2]BF_4$	240	5.5 (*R*)
9[a]	$[Rh(COD)Cl]_2$	28	64.8 (*S*)
10	$[Rh(COD)Cl]_2$	20	74 (*S*)

[a] F. Agbossou-Niedercorn, unpublished results.

The reality of neutral Rh-dihydride-chloride complexes has been shown through the use of PHIP NMR techniques. Indeed, Eisenberg found a way to detect new mononuclear neutral dihydride-rhodium-phosphane-olefin complexes that appear to be intermediates in the catalytic hydrogenation of olefins (Scheme 3).[37]

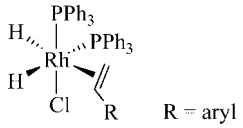

Scheme 3. Schematic representation of the neutral Rh-dihydride-chloride complex.

On the basis of these data, a plausible catalytic cycle depicted in Scheme 4 has been proposed for the hydrogenation of ketones catalysed by neutral rhodium complexes in aprotic solvents. Hereafter, we will focus on the computation of the various elementary steps of this catalytic cycle.

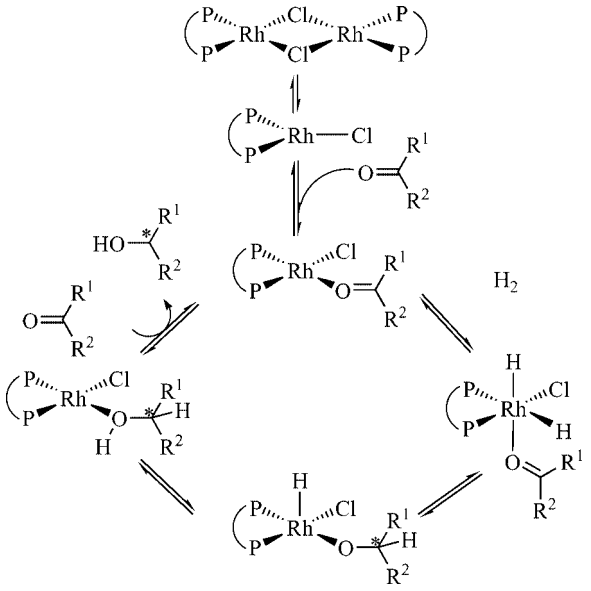

Scheme 4. Proposed reaction mechanism.

Computational Methods

The calculations were based on the density functional theory (DFT) using Becke's three-parameter hybrid functional (B3) and the Lee, Yang and Parr (LYP) correlation functional for the correlation energies (B3LYP). This method[38] exhibits accuracy comparable to that of sophisticated post-Hartree–Fock methods in transition-metal studies. They were performed using the Gaussian 98 program package (version A9).[39] For the rhodium atom, we used the relativist effective core potential of Hay and Wadt (with 4s and 4p in the valence) and the corresponding double-ζ basis set.[40] For the carbon, oxygen, nitrogen and hydrogen atoms of the ligand a 6–3lG* basis set was used. For the hydrogen atoms on the rhodium and those of the reactant (formaldehyde) and product (methanol) a *p*-orbital of Gaussian type ζ = 1.1 was added. For the chlorine and the phosphorus atoms, a 6-311G* basis set was used. All the used basis sets were implemented in the Gaussian 98 program.

Geometries of reactants and products were fully optimised without any symmetry or internal coordinate constrains. All transition states were characterised by determining the number of imaginary frequencies and a further characterisation of the transition state was achieved by calculation of the intrinsic reaction coordinate (IRC) leading to the corresponding reactants and products.

Models Used for the Calculation of the Complexes

The Ligand: The skeleton of the AMPP ligand {(*S*)-Cp^s,Cp^s-oxoProNOP} is replaced by an ethanolamine-bridged diphosphane [$H_2POCH_2CH_2N(H)PH_2$] (Scheme 5). Thus, the electronic effects of the oxygen and nitrogen atoms are maintained. In addition, the CH_2CH_2 spacer provides the constraint on the carbon backbone of the ligand which mimics the skeleton of the pyrrolidine ring present in the most efficient ligands studied. Hydrogen atoms replace the phosphorus substituents in order to reduce computational time.

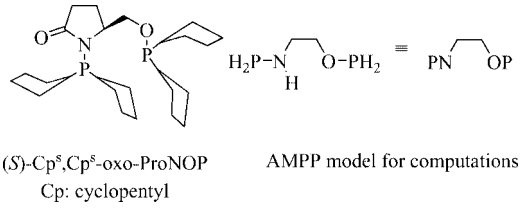

(*S*)-Cp^s,Cp^s-oxo-ProNOP
Cp: cyclopentyl

AMPP model for computations

Scheme 5. AMPP and the model compound.

Ketopantolactone: Calculations were performed by using a model hydrogenation reaction of formaldehyde and when necessary with larger carbonyl compounds.

Computational Results

Coordination of the Substrate: Structures of Catalyst–Substrate Adducts

The d^8 complex [Rh(Cl){PO∩NP}] is a model for the product expected from the cleavage of the dimeric precursor [Rh{PO∩NP}Cl]$_2$ which leads to the formation of the active species. It is well known that ML_3 complexes can be stable in a T-shaped trigonal structure. Nevertheless, the contribution of solvent coordination through a C=C bond providing a square-planar complex has been computed by means of optimisation of Rh(Cl){PO∩NP}(C_6H_6). The calculations show that the coordination energy of a benzene in the η^2 mode is almost thermoneutral (around 2 kcal/mol depending upon the geometry). Consequently, and taking into consideration the results related next, the eventual intermediate square-planar complex bearing a solvent molecule was not considered further in the catalytic cycle.

As T-shaped trigonal complexes present a C_1 symmetry, two isomeric compounds have to be considered that present the chloride either *trans* to P_N (**1a**) or *trans* to P_O (**1b**) (Figure 1). The energy difference between both optimised complexes is very small (0.2 kcal/mol). The activation energy on going from one isomer to the other is only 4.5 kcal/mol. Furthermore, both experimentally and theoretically, the length of the Rh–P_O and Rh–P_N bonds present only a small difference (0.02–0.03 Å experimentally, 0.03 Å by calculation).[41] Because of these small differences, it can be foreseen that the coordination of the carbonyl substrate *trans* of both moieties, i.e., P_O and P_N, will be alike. The relative

stabilities are consistent with a larger *trans* influence of the P_O group, an effect which can be observed in the Rh–Cl bond lengths: 2.348 Å when *trans* to P_N and 2.363 Å when *trans* to P_O.

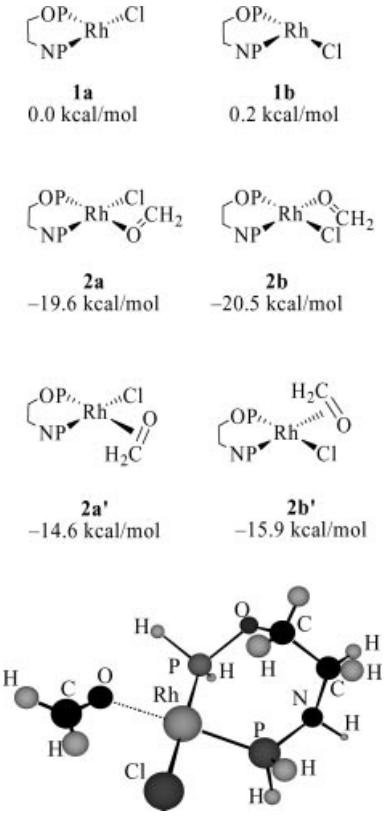

Figure 1. Schematic representation of the intermediates **1** and **2**. Values indicating the relative energies compared to **1a** + CH_2O (top). Geometry of the most stable complex (bottom).

Carbonyl substrates can adopt two fundamental coordination modes on a transition metal complex: end-on coordination (η^1) by a lone pair of the oxygen atom or side-on coordination (η^2) through the CO π system.[42] Both modes have been taken into consideration (Figure 1). The η^1 coordination mode (structures **2a**–**b**) of the substrate provides more stable complexes than the η^2 one (structures **2a′**–**b′**). As anticipated, the *trans* to P_N η^1-coordinated formaldehyde complex **2b** is only slightly more stable than **2a** by 0.9 kcal/mol.

The energy differences between the two coordination modes are due to two main effects of the same importance: the deformation energy of the organic molecule and the orbital interaction. The deformation energy of the organic molecule is more important in the η^2 coordination mode, destabilising the latter. For energetic reasons, the main orbital interaction is between the metal orbital and the CH_2O nonbonding orbital located on the oxygen atom, which is also in favour of the η^1 coordination. Furthermore, as a test, we considered also acetone coordination on complex **1**. Starting with the molecule coordinated in a η^2 coordination mode invariably ends with a displacement towards the η^1 mode. These calculations confirm that the most stable coordination mode on these complexes is η^1. It should be mentioned that coordination energies of the acetone on the T-shape trigonal complexes are similar to those of the model system (18.2 kcal/mol on complex **1a** and 19.4 kcal/mol on **1b** as compared to 19.5 and 20.6 kcal/mol for the formaldehyde coordination).

Addition of Molecular Hydrogen

The next elementary step of the proposed mechanism is the hydrogen addition, leading to the formation of a dihydride intermediate. As both complexes **2a** and **2b** bearing the η^1-coordinated substrate are of equivalent stability, the oxidative addition of molecular hydrogen has to be considered on the two complexes. Furthermore, the oxidative addition of molecular hydrogen to a square-planar complex may occur on either side of the plane, with the molecular hydrogen parallel to either the Rh–P_O or Rh–P_N bond, which leads to eight different dihydrides with *cis* configuration.[15,43] Thus, the addition of molecular hydrogen along eight diastereomeric pathways must be considered in the modelling. These pathways are designated A, B, C, D, E, F, G and H (Figure 2). The search for stable rhodium-dihydrogen intermediates and the transition states for the addition of molecular hydrogen were performed along these pathways. The energy profiles of the approach of molecular hydrogen along the pathways located above and below the square plane are very similar. In fact, the energy difference between the two corresponding transition states (TS) is less than 1.5 kcal/mol. In the TS, the main interaction occurs between the HOMO of the complex (dz^2), which is symmetric with respect to the plane, and the LUMO of the molecular hydrogen (σ*) and is therefore independent from the approaching face. Molecular hydrogen complexes of rhodium are not computed as stable intermediates in the process of oxidative addition of molecular hydrogen to the square planar rhodium complex. As a matter of fact, IRC calculations do not end on such complexes but rather on the dissociated species or on the rhodium-dihydride compounds. Interestingly, the activation energies which lead to the displacement of either the chloride or the carbonyl from the square plane are quite different as this motion generates large electronic barriers due to extensive nuclear reorganisation. Indeed, the out-of-plane displacement of the chloride is ca. 5 kcal/mol more energy demanding than the out-of-plane displacement of the carbonyl moiety. Thus, energeti-

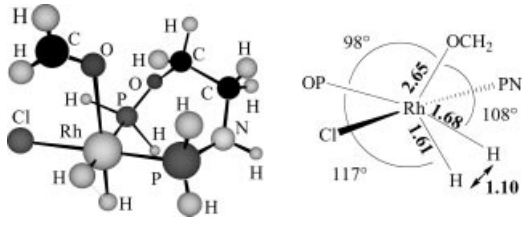

Figure 2. Representation of the transition state between **2a** and **DIHYD-D**.

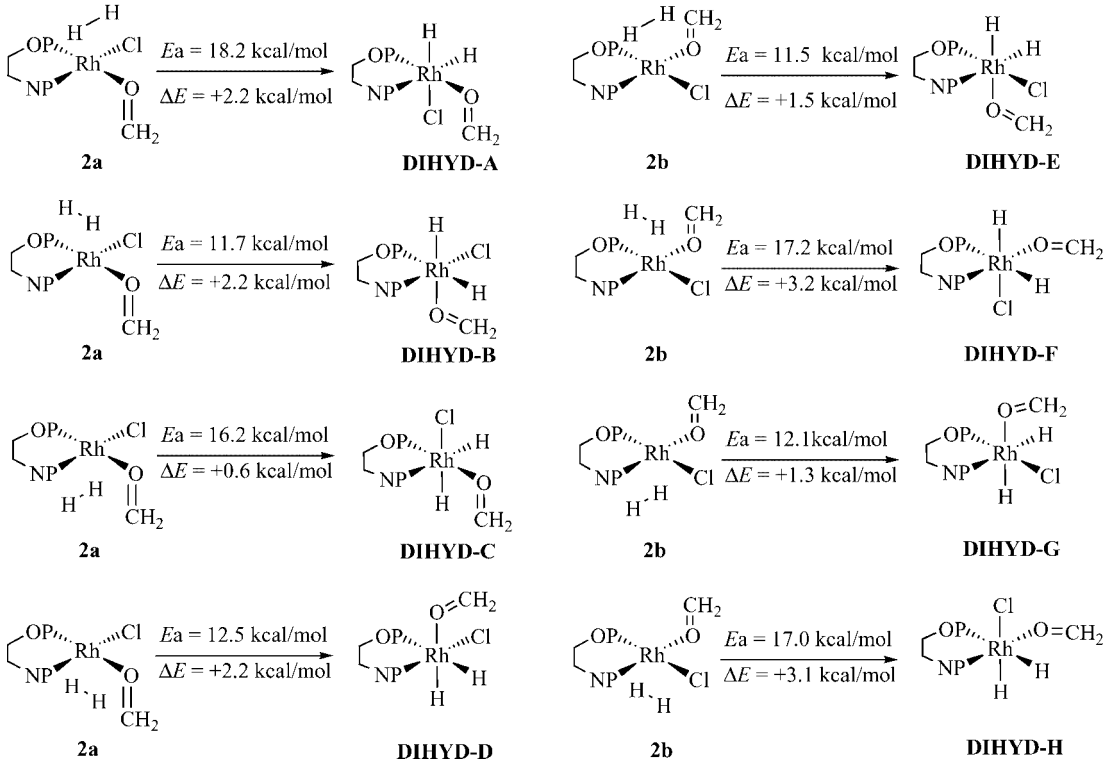

Scheme 6. Reaction and activation energy of the dihydride formation starting from complexes **2a** and **2b**.

cally lower transition states arise from the electronic preference for the chloride to remain in the rhodium-diphosphane plane (Scheme 6).

The transition states in going from **2a** to **DIHYD-B** and **DIHYD-D** and from **2b** to **DIHYD-E** and **DIHYD-G** are favoured. This result supports the final formation of only four isomers under the normal conditions of hydrogenation (room temperature and 1 atm of H_2). The geometries of these four transition states are similar: the H–H bond is almost broken while the Rh–O distance is increased to ca. 2.6 Å. The displaced group (OCH_2) is almost located in its position in the final products. In the case of the formation of **DIHYD-D**, the geometry of the transition state exhibit a H–H distance of 1.10 Å with the O–Rh length of 2.65 Å (Δd = 0.36 Å) (Figure 2). In conclusion, only four dihydride complexes, which result from a *cis* addition of molecular hydrogen, are kinetically accessible minima on the reaction potential surface and are thus viable intermediates. Formation of dihydrides from **2** and molecular hydrogen is ap-

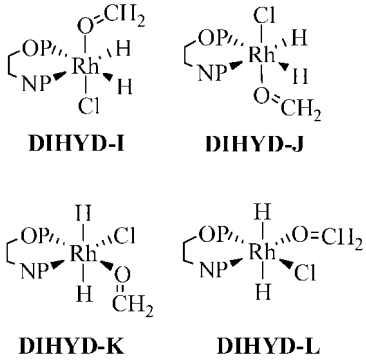

Scheme 7. Schematic representation of the dihydride that cannot be formed in one step, by hydrogen addition on complex **2**.

Table 3. Relative energies of the various intermediates (in kcal/mol).

Initial complex		Substrate coordination		Molecular hydrogen addition		Alkoxide formation		Reductive elimination	
1a	0.0	**2a**	+0.7	DIHYD-A	+1.6				
				DIHYD-B	+1.8	**4b**	+0.3	**5b**	+5.2
				DIHYD-C	0.0				
				DIHYD-D	+1.5	**4d**	+0.8		
1b	+0.2	**2b**	0.0	DIHYD-E	+0.3	**4e**	0.0	**5e**	0.0
				DIHYD-F	+2.0				
				DIHYD-G	+0.1	**4g**	+2.5		
				DIHYD-H	+1.9				
1a		**2a′**	+5.7	DIHYD-I	+19.2				
1b		**2b′**	+4.6	DIHYD-J	+20.4				
				DIHYD-K	+19.5				
				DIHYD-L	+18.0				

proximately thermoneutral; reaction enthalpies range from 0.6 to 3.2 kcal/mol.

The complexes possessing either *trans* hydrides or the chlorine and carbonyl in apical positions gave structures much less stable by 18.0 to 20.4 kcal/mol. The transition states to those improbable species have not been studied and these intermediates have not been further considered in the calculations (Scheme 7), as their formation activation energies will be larger than 20 kcal/mol. The relative energies of all intermediates are given in Table 3.

Transfer of the First Hydride: Conversion of the Dihydrides into Alkoxy Hydrides via Migratory Insertion

A variety of alkoxy hydrides can be obtained by migratory insertion of the C=O bond into the Rh–H bond of a dihydride. As mentioned above, we did not consider structures presenting a *trans* arrangement of the dihydrides nor the structures presenting the *cis* arrangement of the dihydrides in the plane defined by the Rh and the two P atoms; not because they could not give insertion products but because of the improbable participation of such species in the hydrogenation process. The alkoxy formation starting from dihydride without the Cl atom in the RhPP plane has also not been considered as they are much more slowly formed. In conclusion, only the four dihydride complexes **DIHYD-B**, **DIHYD-D**, **DIHYD-E** and **DIHYD-G** have been taken into consideration for this step (Scheme 8). They present *cis* coplanar orientations of the coordinated C=O and one Rh–H being systematically located in the plane containing the diphosphane ligand. The activation energies are reported in Scheme 8 and the relative energies of the obtained intermediates in Table 3. The transition state corresponds to the intramolecular hydride transfer of a H atom into the C–Rh bond that could be created in the case of a η^2 coordination mode. However, it is not the H atom, which moves toward the C atom, but the opposite. After the H addition, the complexes have an empty coordination site that can be located either in a *trans* position to the H atom or in a *trans* position to one of the phosphorus atoms. The latter geometries are not stable and evolve without activation energies to the one possessing the emty coordination site *trans* to the H atom. The geometry of one transition state is represented in Figure 3.

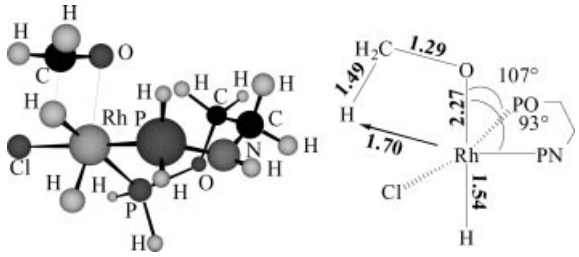

Figure 3. Transition-state geometry for the conversion of **DIHYD-D** into **4d**.

An IRC calculation was carried out for one of the transition-state structures. The final points are, on one side, the 18-electron starting complex with the C=O in a η^2 coordination mode, and on the other side, a complex with the alkoxy species. This calculation suggests that the substrate changes from a η^1 coordination to a η^2 coordination just prior to hydride insertion. The activation energy of this isomerisation is only 4.8 kcal/mol, the resulting dihydride being less stable than the starting one by 3.6 kcal/mol. This step will become improbable with larger carbonyl substrates. For this reason, we have not decomposed the C–H bond formation into two steps in the energetic diagram. This almost elementary step is slightly exothermic (ΔE: –1.4 to –4.7 kcal/mol). The stable intermediates have square-planar pyramidal structures with the alkoxy fragment located in the square plane. The resulting stable structures all have a *cis* arrangement of the remaining H and alkoxy moieties. The site in the *trans* position to the H ligand is empty.

Conversion of the Alkoxy Hydride into the Hydroxy Complex: Reductive Elimination

The next step is the reductive elimination starting from the four intermediates (**4b**, **4d**, **4e**, **4g**) (Scheme 9). The reductive elimination of the alkoxy hydride provides a square-

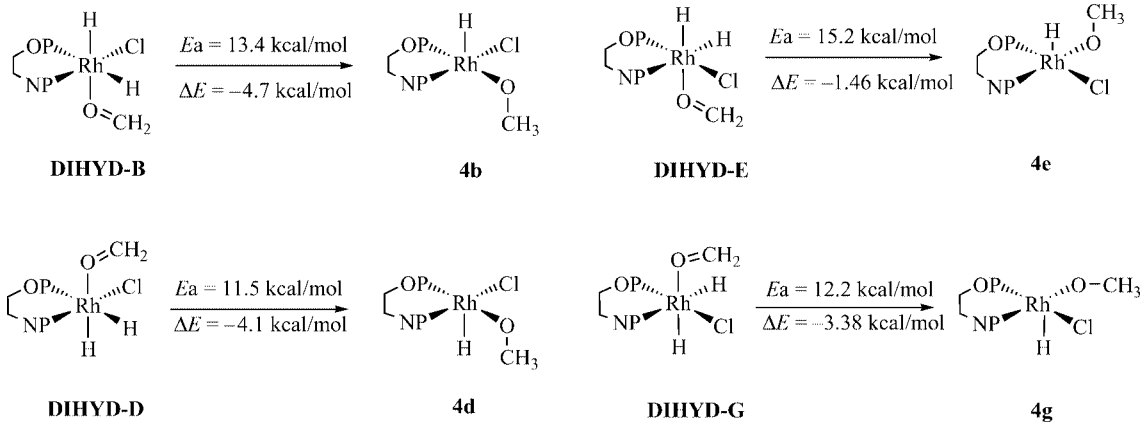

Scheme 8. Reaction and activation energies for the alkoxy formation.

planar structure in which the hydroxy species is coordinated to the rhodium.

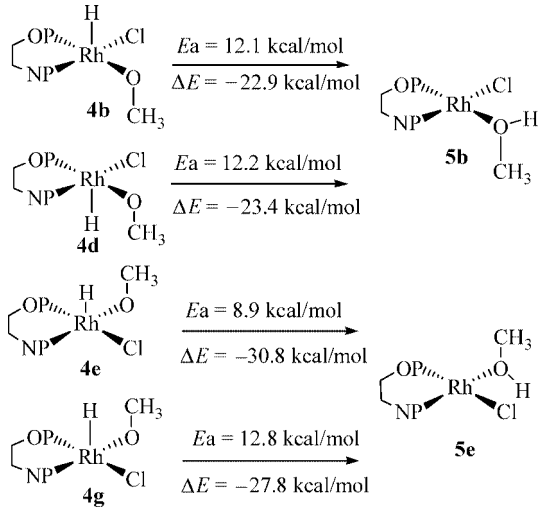

Scheme 9. Reaction and activation energies for the formation of the alcohol.

This structure is closely related to the starting complexes bearing the coordinated substrate C=O. Two structures are obtained with the hydroxy located either *trans* to the P_O moiety or *trans* to the P_N end. The energies are slightly in favour of a *trans* to P_N location as in the case of the complexes resulting from the first step, i.e., coordination of the substrate.

The calculation indicates that the process of reductive elimination resulting in the reduction of Rh^{III} to Rh^{I} is highly exothermic (from –22.9 to –30.0 kcal/mol) (Scheme 9). The reaction coordinate is constituted almost exclusively by the H–Rh–O angle, which decreases from 90° to 15°. The transition state is reached for a value of that angle close to 50° (Figure 4). The activation energy is smaller than 13 kcal/mol for the four reactions path we have studied.

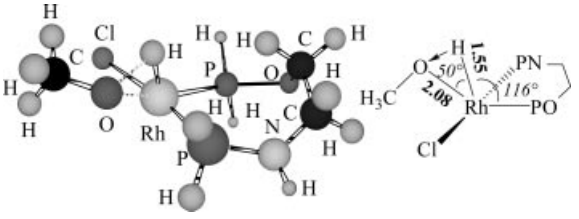

Figure 4. Representation of the transition state between **4b** and **5b**.

Because of the similar energies of the C=O-coordinated structures and the hydroxy coordinated one, it is not unreasonable to consider that the reaction could be inhibited by an excess of hydroxy compounds which might occur in high conversions of the hydrogenation reaction or when the concentration in the produced hydroxy compound becomes higher than that of the ketonic substrate. However, as the partial order of the reaction has not been performed, it is rather difficult to know if such an inhibition effect is observed experimentally.

Alcohol-Carbonyl Substrate Substitution

In the catalytic cycle, the last step is a substitution of the hydroxy compound by the carbonyl substrate. This step is almost athermic: slightly exothermic from **5b** and slightly endothermic from **5e** (Scheme 10) and can take place in one step (concerted mechanism). In the transition state, the two Rh–O distances are almost the same [2.60 Å for Rh–O(hydroxy) and 2.54 Å for Rh–O (carbonyl)] (Figure 5). The activation energy of that step is small (5.6 kcal/mol, Scheme 10). An alternative mechanism would be the associative one. However, the reaction involving the carbonyl coordination prior to hydroxy rhodium bond cleavage is an overall endothermic process and the energy loss is similar to the activation energy of the direct exchange reaction, indicating that the substitution should occur in one step.

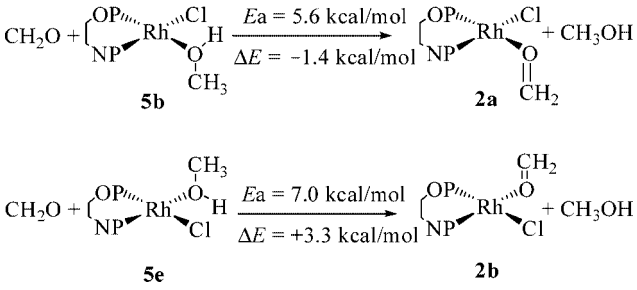

Scheme 10. Reaction and activation energies for the ligand exchange.

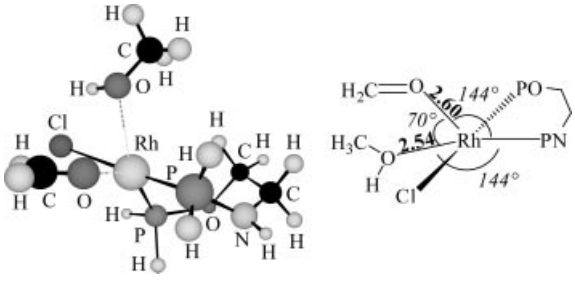

Figure 5. Transition-state geometry for the CH_3OH/CH_2O exchange reaction.

Catalytic Cycle

Figure 6 and Figure 7 present the calculated energy profile for the entire catalytic cycle starting from the two complexes presenting the carbonyl substrate in a *trans* position to **2a** or **2b**. All activation energies are reported on the Figures. The energy difference between the final state (**2** + methanol) and the initial state (**2** + formaldehyde + H_2) of the cycle is the energy of hydrogenation of formaldehyde. The overall energy profile is smooth. This reaction is highly exothermic. The migratory insertion step [from **2** to the **DIHYD-D** complexes has the most important activation barrier (12.5 kcal/mol)] and might be considered as the rate-limiting step. For the two types of complexes, for steric in-

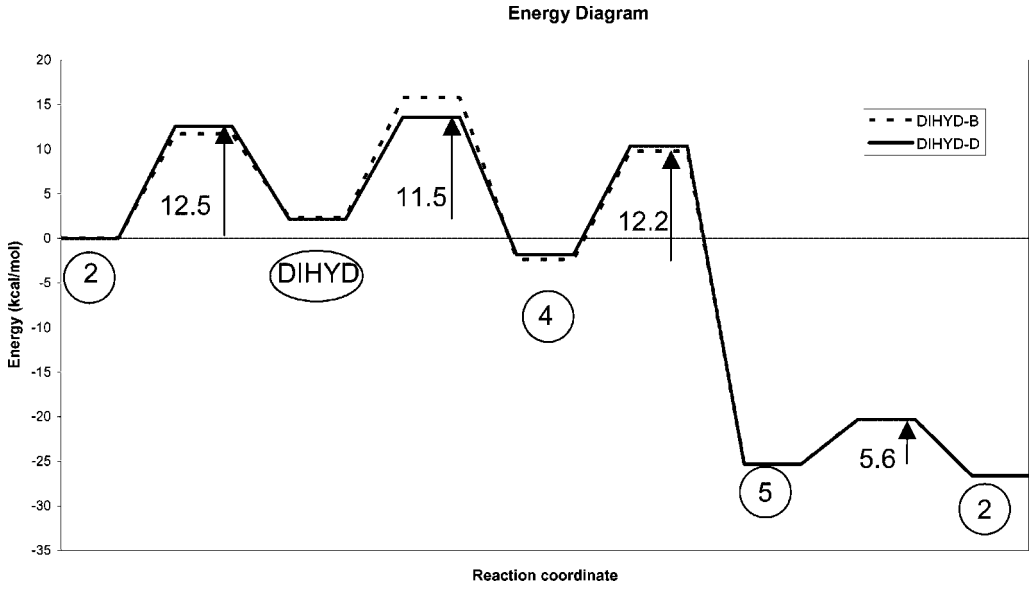

Figure 6. Calculated reaction profile (kcal/mol) of the entire catalytic cycle for the hydrogenation of C=O starting from **2a** (the two last stationary points are common for the two reaction paths).

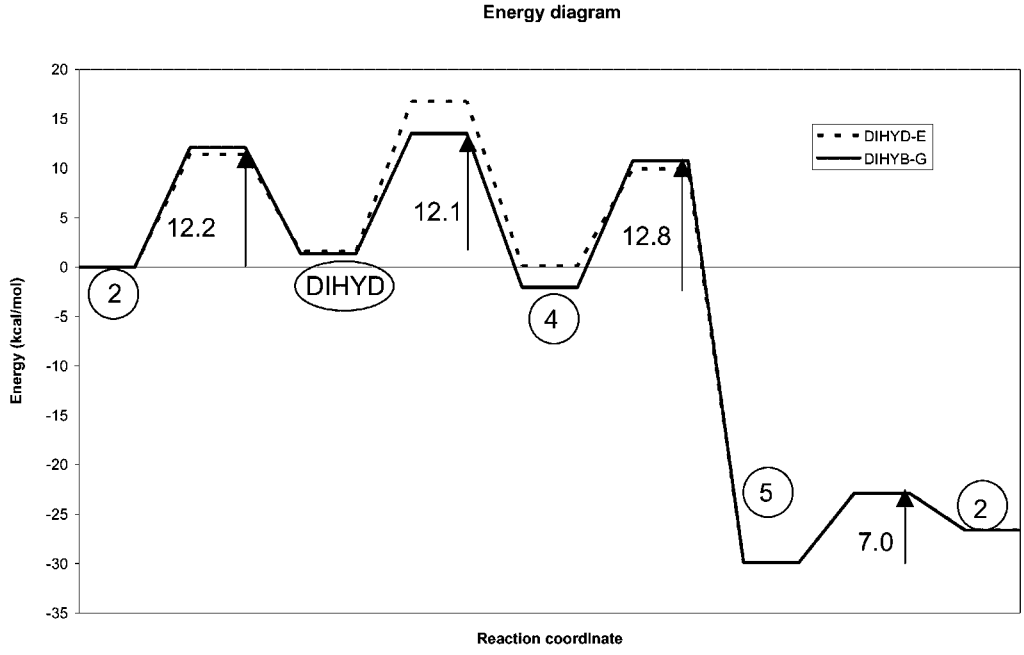

Figure 7. Calculated reaction profile (kcal/mol) of the entire catalytic cycle for the hydrogenation of C=O starting from **2b** (the two last stationary points are common for the two reaction paths).

teraction reasons the C–H formation is favoured when the substrate is located on the same side of the RhPP plane as the C2 chain. These interactions will play an important role for prochiral substrates.

Conclusions

In this paper, we have presented the possible pathways of the mechanism of hydrogenation of C=O bonds catalysed by neutral rhodium complexes employing the B3LYP density functional method. This theoretical study is the first one carried out on neutral rhodium-based C=O bond hydrogenation. Our purpose was to calculate the most probable pathway for the catalytic reaction. Thus, new insight into our understanding of the reaction is provided here. We performed geometry optimisation for all isomers of intermediates and transition states. Eight diastereomeric pathways have been followed for the *cis* addition of molecular hydrogen to [Rh{$H_2POCH_2CH_2N(H)PH_2$}(CI)(H_2CO)] leading to eight distinct isomeric dihydride intermediates. The postulated intermediates are minima on the potential surface. Four resulting dihydride complexes have been con-

sidered as the more accessible intermediates. In addition, we showed that even if one isomer can be considered as the most stable within a series, several isomeric structures are able to be involved in every step of the cycle and have to be examined in future studies. For formaldehyde hydrogenation, the rate-determining step is difficult to determine on the basis of the energy diagram. However, the calculation of one similar energy path for methanal and propanone indicate that the migratory path of hydride to the carbonyl moiety is the rate-determining step.[44] The overall energy profile of the catalytic cycle is smooth and corresponds to an exothermic process. On the basis of experimental data and on calculations, the hydrogenation of ketones with the participation of only neutral catalytic intermediates bearing a chloride atom during the entire process and without chelation of the substrate is thus likely to proceed. This is strongly supported by the efficiency of such catalysts in the highly efficient hydrogenation of even simple ketones under neutral conditions.[29]

Acknowledgments

The authors thank Prof. André Mortreux for fruitful discussions and Dr. Corinne Pasquier for preliminary experimental results. We also thank the Centre National de la Recherche Scientifique and the Ministère de la Recherche et de la Technologie for financial support. Finally, we thank CRI (Centre des Ressources Informatiques) of the Université des Sciences et Technologies de Lille (partially founded by FEDER) for their computational support.

[1] a) R. Noyori, *Asymmetric Catalysis in Organic Synthesis*, Wiley, New York, **1994**, ch. 2, pp. 16–94; b) H. Takaya, T. Ohta, R. Noyori, *Catalytic Asymmetric Synthesis* (Ed.: I. Ojima), VCH Publishers, New York, **1993**, chapter 3, pp. 1–39; c) T. Ohkuma, M. Kitamura, R. Noyori, *Catalytic Asymmetric Synthesis*, 2nd ed. (Ed.: I. Ojima), VCH Publishers, New York, **2000**, chapter 1, pp. 1–110.

[2] R. Noyori, T. Ohkuma, *Angew. Chem.* **2001**, *113*, 40–73; *Angew. Chem. Int. Ed.* **2001**, *40*, 40–73.

[3] a) R. Schmid, *Chimia* **1996**, *50*, 110–113; b) R. Schmid, E. A. Broger, *Abstract of Chiral Europe 94*, Nice, September **1994**.

[4] a) H.-U. Blaser, F. Spindler, M. Studer, *Appl. Catal., A* **2001**, *221*, 119–143; b) S. C. Stinson, *Chem. Eng. News* **1999**, *77*, 101–120; c) H. U. Blaser, B. Pugin, F. Spindler, *Applied Homogeneous Catalysis with Organometallic Compounds* (Eds.: B. Cornils, W. A. Herrmann), 2nd ed., Wiley, New York, **2002**, vol. 3, 1131–1149.

[5] M. J. Palmer, M. Wills, *Tetrahedron: Asymmetry* **1999**, *10*, 2045–2061 and references cited therein.

[6] a) R. Noyori, S. Hashiguchi, *Acc. Chem. Res.* **1997**, *30*, 97–102; b) S. Hashiguchi, A. Kujii, T. Takehara, T. Ikariya, R. Noyori, *J. Am. Chem. Soc.* **1995**, *117*, 7562–7563; c) T. Ohkuma, H. Ooka, T. Ikariya, R. Noyori, *J. Am. Chem. Soc.* **1995**, *117*, 10417–10418.

[7] A. S. C. Chan, J. J. Pluth, J. Halpern, *J. Am. Chem. Soc.* **1980**, *102*, 5952–5954.

[8] J. M. Brown, R. A. Chaloner, *J. Chem. Soc., Chem. Commun.* **1980**, 344–346.

[9] C. Landis, J. Halpern, *J. Am. Chem. Soc.* **1987**, *109*, 1746–1754.

[10] J. M. Brown, *Hydrogenation of Functionalized Carbon-Carbon Double Bonds* (Eds.: E. N. Jacobsen, A. Pfaltz, H. Yamamoto), Springer, Berlin, **1999**, vol. l, pp. 119–182.

[11] J. Halpern, D. P. Riley, A. S. C. Chan, J. J. Pluth, *J. Am. Chem. Soc.* **1977**, *99*, 8055–8057.

[12] A. S. C. Chan, J. Halpern, *J. Am. Chem. Soc.* **1980**, *102*, 838–840.

[13] a) A. S. C. Chan, J. Pluth, J. Halpern, *Inorg. Chim. Acta* **1979**, *37*, 477–479; b) J. Halpern, *Science* **1982**, *217*, 401–407.

[14] I. Gridnev, N. Hagashi, K. Asakura, T. Imamoto, *J. Am. Chem. Soc.* **2000**, *122*, 7183–7194 and references cited therein.

[15] a) C. R. Landis, P. Hilfenhaus, S. Feldgus, *J. Am. Chem. Soc.* **1999**, *121*, 8741–8754; b) S. Feldgus, C. R. Landis, *Organometallics* **2001**, *20*, 2374–2386; c) S. Feldgus, C. R. Landis, *J. Am. Chem. Soc.* **2000**, *122*, 12714–12727; d) C. R. Landis, S. Feldgus, *Angew. Chem.* **2000**, *112*, 2985–2988; *Angew. Chem. Int. Ed.* **2000**, *39*, 2863–2866; e) A. Kless, A. Börner, D. Heller, R. Selke, *Organometallics* **1997**, *16*, 2096–2100.

[16] J. S. Giovannetti, C. M. Kelly, C. R. Landis, *J. Am. Chem. Soc.* **1993**, *115*, 4040–4057.

[17] K. Rossen, *Angew. Chem.* **2001**, *113*, 4747–4749; *Angew. Chem. Int. Ed.* **2001**, *40*, 4611–4613.

[18] a) R. Eisenberg, *Acc. Chem. Res.* **1991**, *24*, 110–116; b) J. Bargon, *Applied Homogeneous Catalysis with Organometallic Compounds* (Eds.: B. Cornils, W. A. Herrmann), VCH, Weinheim, **1996**, vol. 2, pp. 672–683.

[19] A. Harthun, R. Kadyrov, R. Selke, J. Bargon, *Angew. Chem.* **1997**, *109*, 1155–1156; *Angew. Chem. Int. Ed. Engl.* **1997**, *36*, 1103–1105.

[20] R. Giernoth, H. Heinrich, N. J. Adams, R. J. Deeth, J. Bargon, J. M. Brown, *J. Am. Chem. Soc.* **2000**, *122*, 12381–12382 and references cited therein.

[21] a) V. Guiral, F. Delbecq, P. Sautet, *Organometallics* **2001**, *20*, 2207–2214; b) M. Bernard, V. Guiral, F. Delbecq, F. Fache, P. Sautet, M. Lemaire, *J. Am. Chem. Soc.* **1998**, *120*, 1441–1446; c) V. Guiral, F. Delbecq, P. Sautet, *Organometallics* **2000**, *19*, 1589–1598.

[22] G. Zassinovitch, G. Mestroni, S. Gladiali, *Chem. Rev.* **1992**, *92*, 1051–1069.

[23] a) D. A. Alonso, P. Brandt, S. J. M. Nordin, P. G. Andersson, *J. Am. Chem. Soc.* **1999**, *121*, 9580–9588; b) M. Yamakawa, H. Ito, R. Noyori, *J. Am. Chem. Soc.* **2000**, *122*, 1466–1478.

[24] R. R. Schrock, J. A. Osborn, *J. Chem. Soc. C* **1970**, 567–568.

[25] Q. Jiang, Y. Jiang, D. Xiao, P. Cao, X. Zhang, *Angew. Chem.* **1998**, *110*, 1203–1207; *Angew. Chem. Int. Ed.* **1998**, *37*, 1100–1103.

[26] I. Ojima, T. Kogure, K. Achiwa, *J. Chem. Soc., Chem. Commun.* **1977**, 428–430.

[27] I. Ojima, T. Kogure, *J. Organomet. Chem.* **1980**, *195*, 239–248.

[28] a) F. Agbossou, J.-F. Carpentier, C. Hatat, N. Kokel, A. Mortreux, P. Betz, R. Goddard, C. Krüger, *Organometallics* **1995**, *14*, 2480–2489; b) F. Agbossou, J.-F. Carpentier, F. Hapiot, I. Suisse, A. Mortreux, *Coord. Chem. Rev.* **1998**, *178–180*, 1615–1645; c) C. Pasquier, S. Naili, A. Mortreux, F. Agbossou, L. Pélinski, J. Brocard, J. Eilers, I. Reiners, V. Peper, J. Martens, *Organometallics* **2000**, *19*, 5723–5732.

[29] a) Y. Kuroki, D. Asada, K. Iseki, *Tetrahedron Lett.* **2000**, *41*, 9853–9858; b) Y. Kuroki, Y. Sakamaki, K. Iseki, *Org. Lett.* **2001**, *3*, 457–459.

[30] a) G. Surpateanu, F. Agbossou, J.-F. Carpentier, A. Mortreux, *Tetrahedron: Asymmetry* **1998**, *9*, 2259–2270; b) F. Agbossou, J.-F. Carpentier, A. Mortreux, G. Surpateanu, A. J. Welch, *New J. Chem.* **1996**, *20*, 1047–1060.

[31] A complete chemical Review issue has been devoted to computational transition chemistry: *Chem. Rev.* **2000**, *100*, 351–801. For recent examples of computation on catalytic reactions, see ref.[21,23].

[32] C. Hatat, A. Karim, N. Kokel, A. Mortreux, F. Petit, *New J. Chem.* **1990**, *14*, 141–152.

[33] N. Keiken, P. Pregosin, G. Trabesinger, *Organometallics* **1998**, *17*, 4510–5518.

[34] J. Bakos, I. Toth, B. Heil, G. Szalontai, L. Parkanyi, V. Fulop, *J. Organomet. Chem.* **1989**, *370*, 263–276.

[35] Dielectric constants taken from the Handbook of Chemistry and Physics, benzene $\varepsilon = 2.284$, methanol $\varepsilon = 33.62$.

[36] a) A. Roucoux, M. Devocelle, J.-F. Carpentier, F. Agbossou, A. Mortreux, *Synlett* **1995**, 358–360; b) A. Roucoux, L. Thieffry, J.-F. Carpentier, M. Devocelle, C. Méliet, F. Agbossou, A. Mortreux, A. J. Welch, *Organometallics* **1996**, *15*, 2440–2449.
[37] S. B. Duckett, C. L. Newell, R. Eisenberg, *J. Am. Chem. Soc.* **1994**, *116*, 10548–10556.
[38] a) A. D. Becke, *J. Chem. Phys.* **1993**, *98*, 5648–5652; b) C. Lee, W. Yang, R. G. Parr, *Phys. Rev. B* **1988**, *37*, 785–789.
[39] A. D. Daniels, K. N. Kudin, M. C. Strain, O. Farkas, J. Tomasi, V. Barone, M. Cossi, R. Cammi, B. Mennucci, C. Pomelli, C. Adamo, S. Clifford, J. Ochterski, G. A. Petersson, P. Y. Ayala, Q. Cui, K. Morokuma, D. K. Malick, A. D. Rabuck, K. Raghavachari, J. B. Foresman, J. Cioslowski, J. V. Ortiz, A. G. Baboul, B. B. Stefanov, G. Liu, A. Liashenko, P. Piskorz, I. Komaromi, R. Gomperts, R. L. Martin, D. J. Fox, T. Keith, M. A. Al-Laham, C. Y. Peng, A. Nanayakkara, M. Challacombe, P. M. W. Gill, B. Johnson, W. Chen, M. W. Wong, J. L. Andres, C. Gonzalez, M. Head-Gordon, E. S. Replogle, J. A. Pople, Gaussian, Inc., Pittsburgh, PA, **1998**.
[40] P. J. Hay, W. R. Wadt, *J. Chem. Phys.* **1985**, *82*, 299–310.
[41] The length difference between Rh–PO and Rh–PN bonds was obtained from structures described in ref.[28] where references towards other complexes are also given.
[42] References for isolated aldehyde and ketone complexes: N. Quiros-Méndez, J. W. Seyler, A. M. Arif, J. A. Gladysz, *J. Am. Chem. Soc.* **1993**, *115*, 2323–2334. Theoretical studies: a) F. Delbecq, P. Sautet, *J. Am. Chem. Soc.* **1992**, *114*, 2446–2455; b) J. Joubert, F. Delbecq, *J. Organomet. Chem.* **2006**, *691*, 1030–1038.
[43] a) J. M. Brown, P. L. Evans, *Tetrahedron* **1988**, *44*, 4905–4916; b) P. L. Bogdan, J. J. Irwin, B. Bosnich, *Organometallics* **1989**, *8*, 1450–1453.
[44] For the calculation with acetone, the rate-determining step is clearly the hydride migration (ΔEa = 11 kcal/mol).

Received: April 4, 2006
Published Online: September 5, 2006

